remote sensing

MDPI

Correction

Correction: Martinez et al. Neural Network Approaches to Reconstruct Phytoplankton Time-Series in the Global Ocean. *Remote Sens.* 2020, *12*, 4156

Elodie Martinez [1,*], Anouar Brini [1], Thomas Gorgues [1], Lucas Drumetz [2], Joana Roussillon [1], Pierre Tandeo [2], Guillaume Maze [1] and Ronan Fablet [2]

[1] Laboratoire d'Océanographie Physique et Spatiale (LOPS), IUEM, University Brest-CNRS-IRD-Ifremer, 29200 Brest, France
[2] IMT Atlantique, Lab-STICC, UMR CNRS 6285, 29200 Brest, France
* Correspondence: elodie.martinez@ird.fr

The authors wish to make the following corrections to the paper [1]. In this manuscript [1] we investigated the ability of two machine learning methods (a Support Vector Regression-SVR, and a Multi-Layer Perceptron-MLP) to reconstruct satellite surface Chlorophyll-a concentration (Chl) based on physical predictors from oceanic satellite observations and atmospheric reanalysis. Among the predictors used, we considered geographical information through the cosinus and sinus of longitude and the sinus of latitude. A mistake has been made in keeping the geographical positions in degrees whereas they should have been converted into radians.

This error induces an overall increase in the performance of all methods. However, the hierarchy between each method and their specific skills, which is one of the main points discussed in our study, is not altered. Therefore, the main findings remain unchanged:

- Earlier efforts in literature relying on the SVR were only applied to numerical model data and put aside the question of whether different algorithms may have specific behaviors. Here, we show that (1) this learning-based approach can also be applied to satellite observations and (2) can even be further improved through the use of a neural network.
- The use of an MLP also removes computational restrictions regarding the size of the training dataset as imposed by the SVR. As such, SVR could not make the most of available observation datasets.
- The MLP, thanks to its ability to capture complex non-linear relationships, still outperform the SVR to retrieve both Chl spatial and temporal patterns.

The authors apologize for any inconvenience caused and state that the scientific conclusions are unaffected. The original publication has also been updated.

According to the error mentioned above, the following contents should be corrected to the paper.

1. Table Correction

The content in the last line of Table 1 has been corrected as follows:

check for updates

Citation: Martinez, E.; Brini, A.; Gorgues, T.; Drumetz, L.; Roussillon, J.; Tandeo, P.; Maze, G.; Fablet, R. Correction: Martinez et al. Neural Network Approaches to Reconstruct Phytoplankton Time-Series in the Global Ocean. *Remote Sens.* 2020, *12*, 4156. *Remote Sens.* **2022**, *14*, 5669. https://doi.org/10.3390/rs14225669

Received: 17 October 2022
Accepted: 20 October 2022
Published: 10 November 2022

Publisher's Note: MDPI stays neutral with regard to jurisdictional claims in published maps and institutional affiliations.

Table 1. Physical predictors, their relevance to Chl variability, the products used, and their resolution.

Proxy Used as Predictors	Relevance to Chl Variations and Associated References	Products	Spatio-Temporal Resolutions
SST	Vertical mixing and upwelling [17–20] Impacts on phytoplankton metabolic rates [21]	Reyn_SmithOIv2 SST dataset [22]	Monthly on a 1° × 1° spatial grid
Sea level anomaly	Thermocline/pycnocline depths [11,23,24]	Ssalto/Duacs merged product of CNES/SALP project [25]	Weekly on a 1/3° × 1/3° spatial grid
Zonal and meridional surface winds	Surface momentum flux forcing and vertical motions driven by Ekman pumping [20,26]	Atmospheric model reanalysis ERA interim 4 [27]	Every 5-days on a 0.25° × 0.25° spatial grid
Zonal and meridional surface total currents	Horizontal advective processes [4,28]	OSCAR unfiltered satellite product [29]	Every 5-days on a 0.25° × 0.25° spatial grid
Short-wave radiations	Photosynthetically active radiation	NCEP/NCAR Numerical reanalysis [30]	Daily on a 2° grid
Month (cos and sin)	Periodicity of the day of the year (day 1 is very similar to day 365 from a seasonal perspective) [31]		
Longitude (cos and sin) and Latitude (sin)	Periodicity (longitude 0° = longitude 360°) [31]		

Table 2 has been corrected as follows:

Table 2. Multi-layer perceptron (MLP) predictor's relative importance.

Weight	Predictors
0.471	Sin(lat)
0.246	Sea surface temperature
0.052	Cos(lon)
0.05	Sin(lon)
0.03	Short-wave radiations
0.028	Sin(month)
0.025	Zonal surface wind
0.023	Cos(month)
0.021	Meridional surface wind
0.019	Sea level anomaly
0.018	Zonal surface current
0.017	Meridional surface current

2. Figures Correction

This error affects some of the figures in the article with an overall increase in the performance of all methods (e.g., corrected Figure 2).

According to the correction, the correct Figures 2–6 are as follows.

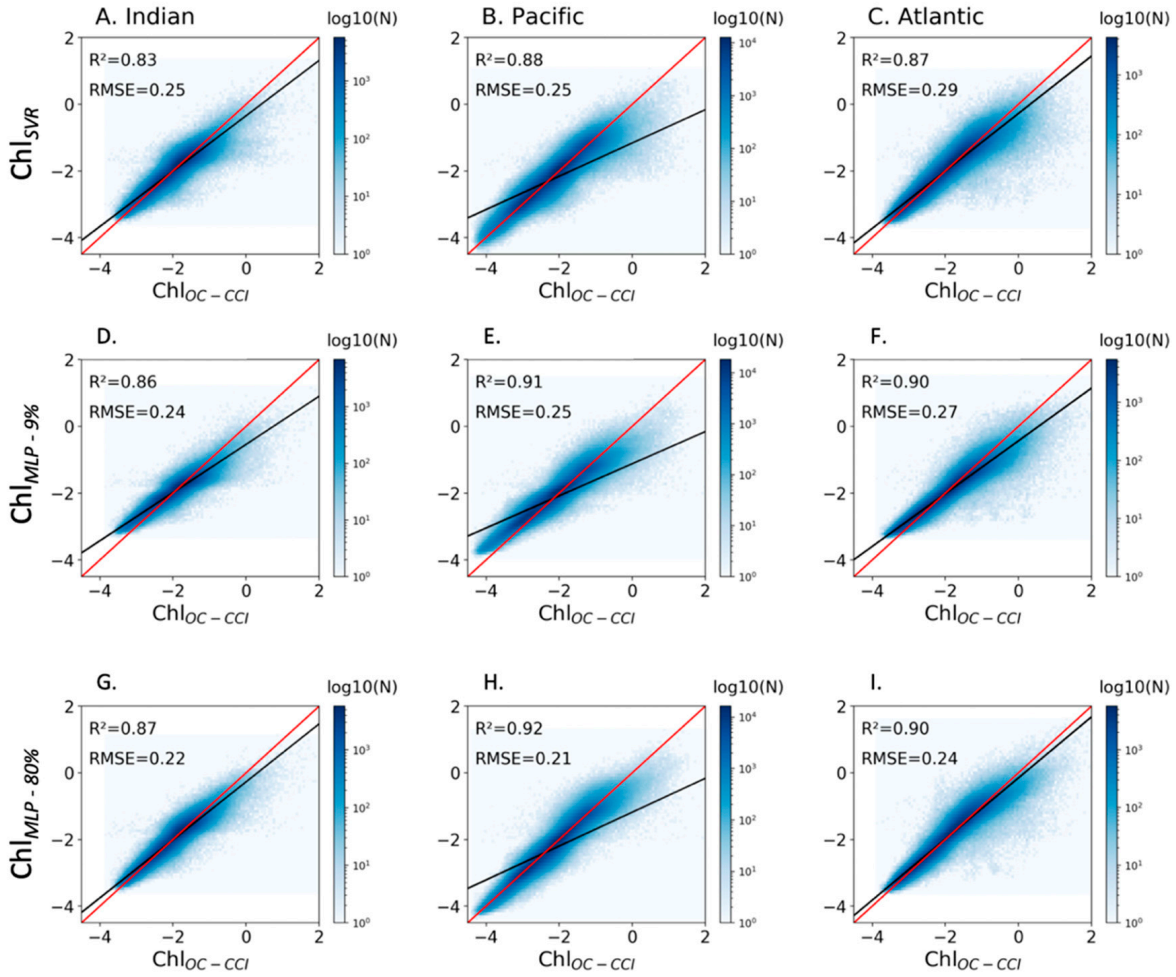

Figure 2. Scatter plots of log of $Chl_{OC\text{-}CCI}$ vs. (**A**–**C**) Chl_{SVR}, (**D**–**F**) $Chl_{MLP\text{-}9\%}$ and (**G**–**I**) Chl_{MLP} trained on 80% of the dataset, for each oceanic basin between 50° S and 50° N and over 1998–2015. The $Chl_{OC\text{-}CCI}$ vs. reconstructed Chl regression lines are plotted in black and the 1:1 regression lines are plotted in red. The figure is color-coded according to the density of observations.

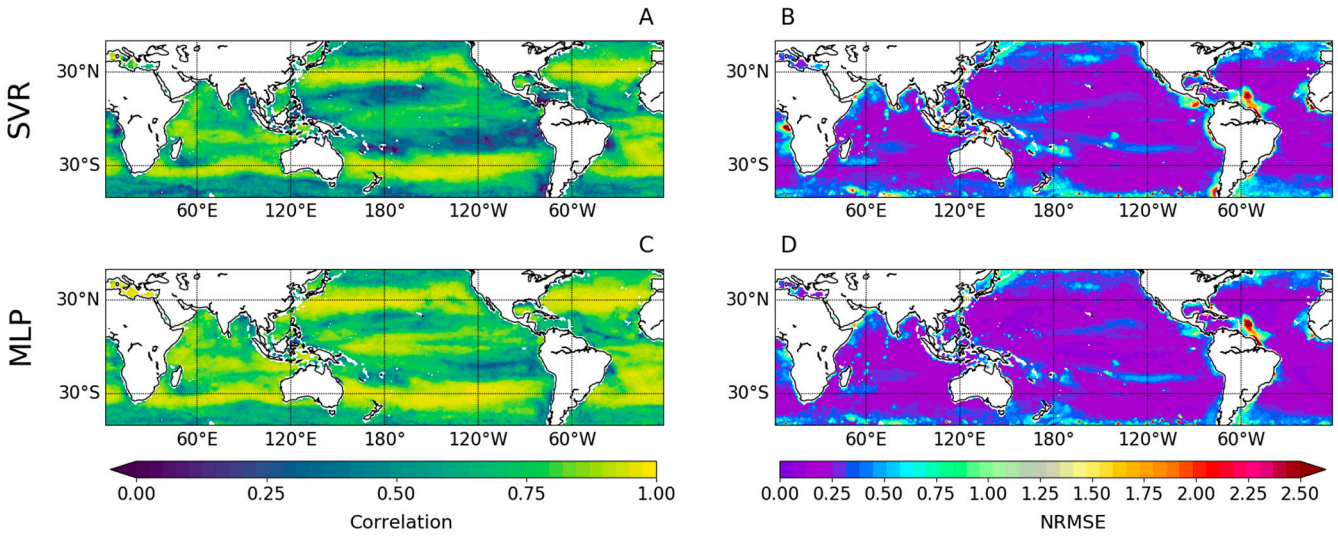

Figure 3. (**A**,**C**) Correlation and (**B**,**D**) NRMSE of $Chl_{OC\text{-}CCI}$ vs. (up) Chl_{SVR} and (bottom) Chl_{MLP} over 1998–2015.

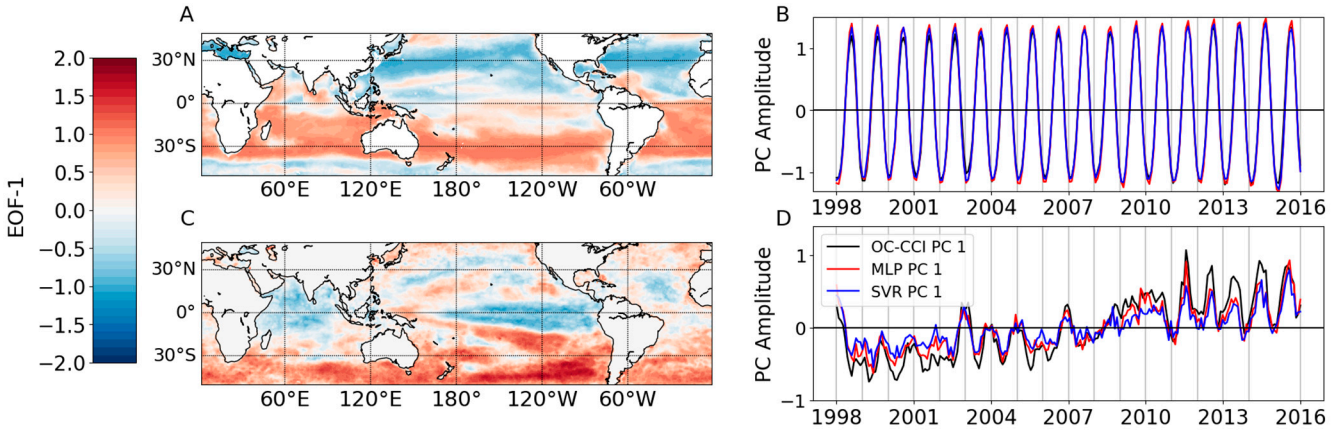

Figure 4. First mode of the $Chl_{OC\text{-}CCI}$ (**A**) seasonal and (**C**) interannual EOFs over 1998–2015, and their associated principal components (**B**,**D**), respectively. Chl_{MLP} and Chl_{SVR} PCs obtained from the $Chl_{OC\text{-}CCI}$ EOF projections are reported in (**B**,**D**).

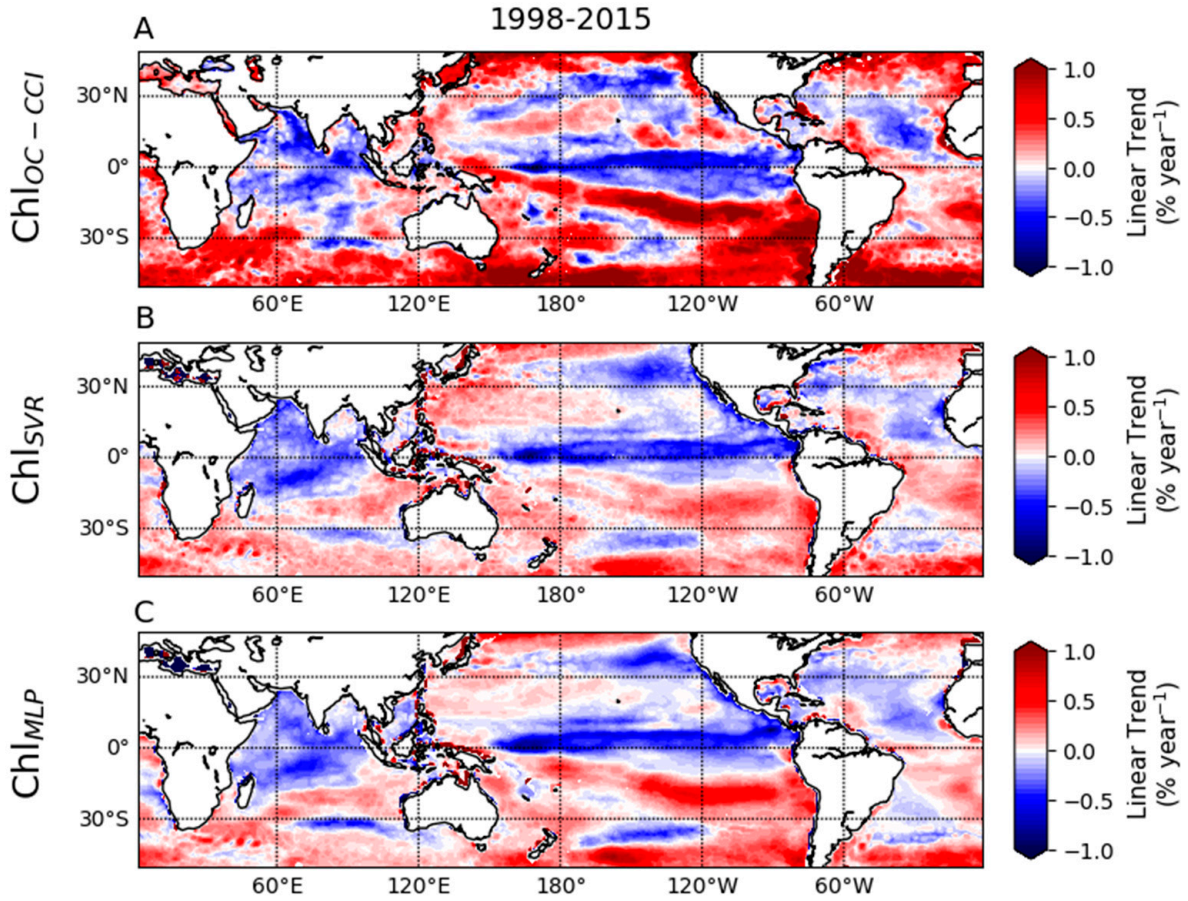

Figure 5. Linear log of (Chl) trend (in % year^{-1}) calculated over 1998–2015 from the monthly (**A**) $Chl_{OC\text{-}CCI}$, (**B**) Chl_{SVR}, (**C**) Chl_{MLP}.

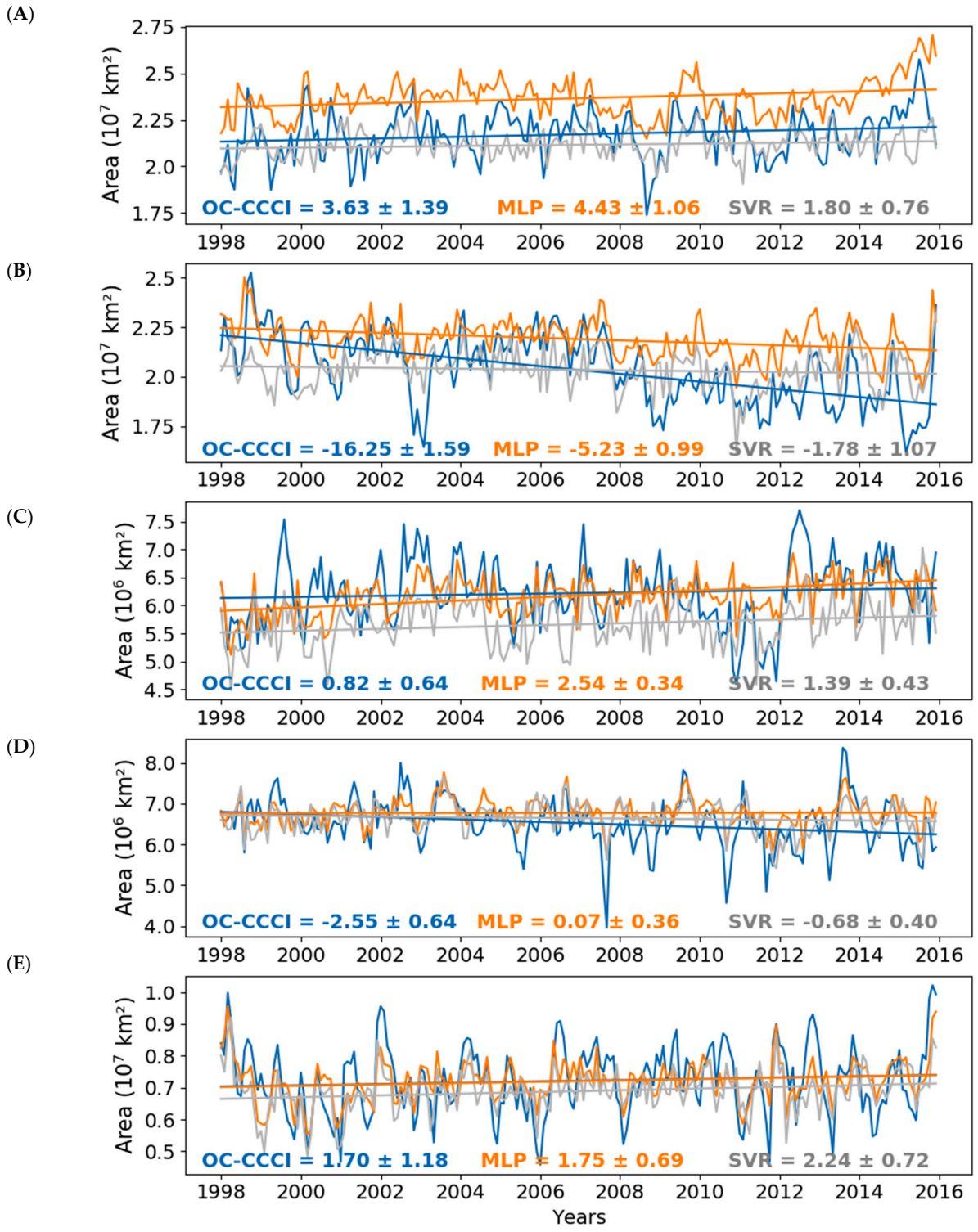

Figure 6. Time series of the monthly mean area (km^2) with surface Chl less than or equal to 0.07 mg.m^{-3} between 5° and 45° N/° S latitude with the seasonal cycle removed in the (**A**) North Pacific, (**B**) South Pacific, (**C**) North Atlantic, (**D**) South Atlantic and (**E**) Indian Oceans. $Chl_{OC\text{-}CCI}$ is in blue, Chl_{SVR} in grey and Chl_{MLP} in orange. Straight lines are the linear trends calculated as in Figure 5. The average trends and standard deviation are also indicated.

3. Text Correction

According to the correction, we updated the related contents in the sections Abstract, 3. Results, 4. Discussion, and Supplementary Materials.

Line 11–15 in Abstract is corrected as:

" . . . The MLP, thanks to its ability to capture complex non-linear relationships, outperforms the SVR to capture satellite Chl spatial patterns (correlation of 0.75 vs. 0.65 on a global scale, respectively) along with its interannual variability and trend, despite an underestimated amplitude. . . . "

Line 1–9 in Paragraph 1 in Section 3.1. is corrected as:

"A first evaluation of the Chl_{SVR} vs. $Chl_{OC\text{-}CCI}$ is provided during 1998–2015 at basin scales and for the whole dataset (Figure 2, upper row). Determination coefficients between both datasets are below 0.88, while RMSE is above 0.25 in the three basins. The MLP trained on the same amount of data than the SVR is more skillful than the SVR at reconstructing $Chl_{OC\text{-}CCI}$ (Figure 2, middle row). Determination coefficients between the log of $Chl_{MLP\text{-}9\%}$ vs. $Chl_{OC\text{-}CCI}$ increase higher than 0.9 in the Atlantic and Pacific oceans, and RMSE are slightly improved. Increasing from 9% to the usual 80%, the MLP training dataset further increases the skills of the NN approach to reconstruct $Chl_{OC\text{-}CCI}$ with a relative gain of 9% to 16% in RMSE and regression lines between the log of Chl_{MLP} vs. $Chl_{OC\text{-}CCI}$ closer to the 1:1 line for each oceanic basin (Figure 2, lower row). . . . "

Line 1–9 in Paragraph 2 in Section 3.1. is corrected as:

"Consistent with the scatterplots, $Chl_{OC\text{-}CCI}$ temporal correlations with Chl_{SVR} are significantly lower than with Chl_{MLP} (Figure 3A,C; r = 0.65 vs. 0.75 and NRMSE = 0.31 vs. 0.26 on a global scale, respectively). $Chl_{OC\text{-}CCI}$ - Chl_{SVR} correlations are higher than 0.8 ($p < 0.001$) over limited regions such as the Atlantic, Indian, and Pacific subtropical areas (Figure 3A). The MLP allows for a significant improvement in the correlation with $Chl_{OC\text{-}CCI}$ with values higher than 0.75 over most of the global ocean (Figure 3C). Areas of high and low NRMSE are similarly distributed for Chl_{SVR} and Chl_{MLP} (Figure 3B,D). For instance, in both cases, NRMSE is higher at the highest latitudes and along the Amazon plume in the Atlantic Ocean. Although the MLP slightly reduces NRMSE compared to the SVR, biases in reference to $Chl_{OC\text{-}CCI}$ still remain in these regions. . . . "

The last two sentences in Paragraph 1 in Section 3.2. are corrected as:

" . . . The seasonal variability of $Chl_{OC\text{-}CCI}$ is well reproduced by both the SVR and MLP (correlations between $Chl_{OC\text{-}CCI}$ and Chl_{SVR} or Chl_{MLP} PCs are both of 0.99; Figure 4B)."

Line 2–5 in Paragraph 2 in Section 3.2. is corrected as:

" . . . Here, the MLP results in an improvement compared with the SVR to reconstruct $Chl_{OC\text{-}CCI}$ inter annual variability, with its first PC correlation with $Chl_{OC\text{-}CCI}$ of 0.95 vs. 0.91 for Chl_{SVR} and amplitude closer to $Chl_{OC\text{-}CCI}$ (Figure 4D)."

Line 2–5 in Paragraph 3 in Section 3.2. is corrected as:

" . . . While most of these trends are captured by Chl_{SVR}, their amplitude is underestimated (Figure 5B). On its side, Chl_{MLP} better reproduces $Chl_{OC\text{-}CCI}$ trends in terms of amplitude, although they remain underestimated (Figure 5C)."

Paragraph 5 in Section 3.2. is corrected as:

"Finally, a first attempt to investigate predictors' relative importance is performed with the MLP approach and a perturbation-based method [60]. Besides latitudes, and as expected, the SST and short-wave radiations are the two most important physical predictors (Table 2). Interestingly, among the physical predictors, the surface wind components seem slightly more important than the sea level anomaly, while this is a common variable used to infer regression between Chl and ocean dynamics [15]. Indeed, redundant indirect information about the ocean circulation can be derived from those predictors, with potentially more information "embedded" within the wind stress that may also be linked to a meaningful parameter for phytoplankton growth: the mixed layer depth. Spatial coordinates, and more specifically the latitude, remain important for the reconstructions, although part of this information is embedded in the spatial patterns of the physical predictors. Indeed, removing spatial information from the MLP training still allows us to reconstruct realistic

Chl, unlike the SVR, which produces unrealistic concentrations, suggesting that the MLP can extract geospatially dependent features from other predictors than the coordinates themselves. The impact of the different predictors on Chl reconstruction according to the oceanic regions and/or the climate cycles should, therefore, be specifically considered and investigated in a dedicated study, once a deep learning scheme will have been considered as sufficiently satisfying."

Line 7–11 in Paragraph 1 in Section 4 is corrected as:

" . . . The MLP demonstrates the ability of deep learning schemes to reproduce satellite Chl with better skill than the SVR, not only to capture the general spatial patterns of Chl but also their interannual signal and trends. Neither the training of the MLP nor that of the SVR involve time information through the training loss which only involves a grid point-wise reconstruction error criterion. . . . "

Line 1–7 in Paragraph 3 in Section 4 is corrected as:

"If, in this study, we demonstrate the better potential of NNs to accurately represent Chl spatial distribution as well as the interannual and trend signals, compared to the SVR, so far, only an MLP was used. MLP is known to not explicitly consider the spatial and temporal correlations in the dataset. Specific architectures to handle spatially or temporally structured data, i.e., convolutional neural networks and recurrent neural networks (such as long short-term memory networks), are currently under investigation and are expected to further improve the Chl reconstruction performance, in particular for the Chl amplitude. . . . "

The following two sentences in Supplementary Materials should be deleted:

"Figure S3: Scatter plots of Chl_{MLP} trained only for predictors with a relative importance higher than 0.1 in Table 2. Figure S4: Correlation and NRMSE of $Chl_{OC\text{-}CCI}$ vs. Chl_{MLP} trained only for predictors with a relative importance higher than 0.1 in Table 2."

4. Supplementary Materials Correction

According to the correction, relevant Figures published in the Supplementary Materials were corrected.

5. Reference Correction

Reference [60] is corrected as: Kim, Y.J.; Kim, H.C.; Han, D.; Lee, S.; Im, J. Prediction of monthly Arctic sea ice concentrations using satellite and reanalysis data based on convolutional neural networks. *Cryosphere* **2020**, *14*, 1083–1104.

Reference

1. Martinez, E.; Brini, A.; Gorgues, T.; Drumetz, L.; Roussillon, J.; Tandeo, P.; Maze, G.; Fablet, R. Neural Network Approaches to Reconstruct Phytoplankton Time-Series in the Global Ocean. *Remote Sens.* **2020**, *12*, 4156. [CrossRef]